Directive Leaky-Wave Radiation From a Dipole Source in a Wire-Medium Slab

Paolo Burghignoli, *Senior Member, IEEE*, Giampiero Lovat, *Member, IEEE*, Filippo Capolino, *Senior Member, IEEE*, David R. Jackson, *Fellow, IEEE*, and Donald R. Wilton, *Life Fellow, IEEE*

***Abstract*—Radiation features are studied for a grounded wire-medium slab excited by a simple canonical source, i.e., a horizontal electric dipole. For the first time, an approximate analysis based on a homogenized model for the wire medium as well as a rigorous full-wave analysis of the actual periodic structure are presented. The homogeneous model takes into account both anisotropy and spatial dispersion of the metamaterial medium in the long-wavelength regime. One rather surprising result is that this structure allows for directive pencil beams at broadside that are azimuthally symmetric (in spite of the directionality of the wires). The structure also allows for conical beams that point at a chosen scan angle, where the beam angle and beamwidth are azimuthally independent, and the beam peak in the elevation planes remains approximately constant during the scanning process, in contrast with other types of planar leaky-wave antennas. These remarkable features are explained in terms of the azimuthal independence of the wavenumber for the leaky mode that is responsible for the beam.**

***Index Terms*—Artificial dielectrics, directive antennas, leaky waves, metamaterials, wire medium.**

I. Introduction

THE possibility to achieve directive radiation from simple sources by employing planar layered structures made of artificial materials has been studied by several research groups, from the early investigations by Gupta and Bahl [1], [2] on slabs hosting periodic layers of metal wires (*wire-medium* slabs) to the more recent ones stimulated by the advent of electronomagnetic bandgap materials and metamaterials [3]–[12].

The wire medium, i.e., a periodic arrangement of parallel infinite metal wires embedded in a host dielectric medium, has been introduced and studied in the 1950s and 1960s [13]–[15] as an artificial dielectric, which exhibits an equivalent plasma-like scalar permittivity in the limit of wavelengths large with respect to the wire spacing and for waves with the electric field polarized along the wire axis. Assuming very thin wires, the currents on them can be assumed to be purely axial, and thus the magnetization is negligible and the medium can be considered non-magnetic.

Manuscript received April 12, 2007; revised October 29, 2007.

P. Burghignoli is with the Department of Electronic Engineering, "La Sapienza" University of Rome, 00184 Rome, Italy (e-mail: burghignoli@die.uniroma1.it).

G. Lovat is with the Department of Electrical Engineering, "La Sapienza" University of Rome, 00184 Rome, Italy (e-mail: giampiero.lovat@uniroma1.it).

F. Capolino is with the Department of Information Engineering, University of Siena, 53100 Siena, Italy.

D. R. Jackson and D. R. Wilton are with the Department of Electrical and Computer Engineering, University of Houston, Houston, TX 77204-4005 USA.

Digital Object Identifier 10.1109/TAP.2008.922620

More recently, the wire medium has been considered as a canonical metamaterial structure, which is actually electrically (uniaxially) anisotropic for arbitrarily-polarized fields. An important result, first pointed out in [16], is that even for large wavelengths the electric response of the wire medium is non-local; hence, a homogeneous model has to take into account not only its anisotropy but also its spatial dispersion, through a dyadic permittivity that explicitly depends on the spatial wavenumbers when expressed in the spectral domain. More complex wire arrangements have also been proposed, e.g., based on finite wires [17], loaded wires [18], or crossed configurations with two or three mutually orthogonal lattices of wires [19]. The homogenization of this kind of media and the relevant effects of spatial dispersion have been studied in depth in [19], [20] for infinite bulk metamaterials and in [21] for metamaterial slabs. Various features of electromagnetic propagation in such media have also been studied, such as propagation of plane waves in unbounded wire media [22] and of surface waves in wire-medium slabs [23].

In [10], a grounded wire-medium slab excited by an electric line source parallel to the wire axis has been considered. In such a 2D configuration a purely TE_{xz} field is excited, with the electric field polarized along the wire axis y, and thus the homogenized metamaterial can be treated as isotropic; conditions for maximizing radiation at broadside and for achieving high broadside directivity have been derived in [10], and they have been shown to be related to the excitation of a weakly-attenuated dominant TE_{xz} leaky mode supported by the grounded metamaterial slab when its equivalent permittivity is positive and much smaller than one. In [24], experimental results on highly-directive antennas based on wire-medium slabs have been presented. In [25] we have compared the leaky-wave model with a pure geometrical-optics analysis. In [26] we have shown the combinations of permittivity-permeability that give rise to high directivity, whereas in [27] a figure of merit has been introduced to compare radiators based on these metamaterial structures with more standard Fabry-Pérot antennas.

In this paper, we extend the analysis of [10] by considering a grounded wire-medium slab excited by an elemental *horizontal electric dipole* parallel to the wire axis (see Fig. 1). In this case the problem is 3D, the excited field is not purely TE_{xz}, and the medium cannot be considered isotropic anymore. A transverse equivalent network (TEN) representation of the structure is derived here, by adopting a spatially-dispersive dyadic permittivity for the homogenized slab and decomposing the spectral field into its TE_y and TM_y parts; the transverse network is then employed to calculate the 3D radiation pattern of the horizontal dipole via the reciprocity theorem. Numerical results

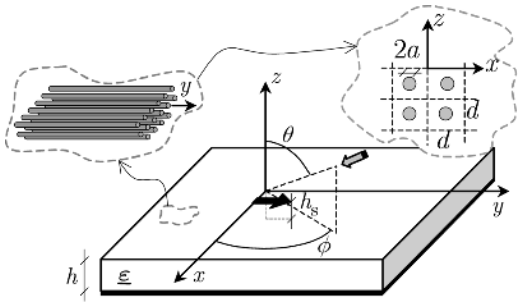

Fig. 1. Grounded wire-medium slab excited by a horizontal electric dipole, with the relevant physical and geometrical parameters; also shown is a uniform plane wave incident from the direction (θ, ϕ), used in the calculation of the far field radiated by the dipole based on the reciprocity theorem.

show various peculiar and interesting features, such as the possibility to achieve narrow omnidirectional beams at broadside, as well as conical scanned beams with equal beam angles and beamwidths in all azimuthal planes. These results are then validated by full-wave simulations of the actual periodic metamaterial structure, performed with a method-of-moments approach that suitably exploits the translational symmetry of the structure along the wire axis in order to reduce the 2.5D problem of plane-wave incidence at oblique angles to a purely 2D problem corresponding to normal incidence.

The propagation characteristics of the dominant TM_y leaky mode (which is responsible for the directive beams) propagating at arbitrary angles along the wire-medium slab are also studied, both with the homogenized model and with the full-wave approach, in order to explain the above-mentioned radiation features. One advantage of the leaky-wave point of view is the possibility to estimate in a simple way the distance at which the structure can be truncated without deteriorating appreciably the radiation properties of the infinite structure, since the attenuation constant of the leaky mode essentially determines the amplitude decay of the field excited in the slab.

The paper is organized as follows. In Section II the transverse network model of the grounded wire-medium slab is presented and used to calculate the 3D far-field pattern of the dipole. In Section III full-wave results for radiation patterns are reported, obtained with the method of moments. In Section IV the scan properties of the conical beam are studied. In Section V the propagation features of the leaky modes supported by the structure are discussed. Finally, in Section VI conclusions are drawn.

II. Analysis Via Homogenization

In this section the wire medium in Fig. 1 is modeled as an effective anisotropic and spatially dispersive homogeneous medium.

The considered structure is made of N layers of periodically-spaced, infinitely-long and perfectly-conducting circular cylinders (wires) (with spatial period d and cylinder radius a) embedded in a host medium with relative permittivity $\varepsilon_{\mathrm{rh}}$ and placed above a perfectly-conducting ground plane. The spacing of the layers is also assumed equal to d, and the distance between the center of the cylinders in the bottom layer and the ground plane is equal to $d/2$. An infinitesimal electric dipole directed along the wire axis y and placed at a distance h_{s} above the ground plane (with $h_{\mathrm{s}} < Nd$) is assumed as a source of the electromagnetic field.

The problem of calculating the far field radiated in an arbitrary direction (θ, ϕ) by the horizontal y-directed electric dipole embedded inside the wire-medium slab can be reduced, by means of the reciprocity theorem, to that of calculating the y-directed electric field produced at the source location by a plane wave impinging on the grounded slab from the same direction [28]. In particular, in the far-field region the component E_p of the electric field (where $p = \theta, \phi$) is written as

$$E_p(r, \theta, \phi) = E_p^{\mathrm{ff}}(\theta, \phi) \frac{e^{-jk_0 r}}{r}. \tag{1}$$

The far-field pattern E_p^{ff} is here calculated via the reciprocity theorem as $E_p^{\mathrm{ff}}(\theta, \phi) = E_y^{\mathrm{pw}}(\theta, \phi)$, where E_y^{pw} is the y component of the electric field at the source location $\mathbf{r} = (0, 0, z_{\mathrm{s}})$ due to a plane wave $\mathbf{E}^{\mathrm{inc}}$ with amplitude $E_0 = -j\eta_0 k_0/(4\pi)$ [28], impinging from the (θ, ϕ) direction, and polarized along $\mathbf{u}_p$:

$$\mathbf{E}^{\mathrm{inc}}(\mathbf{r}) = E_0 \mathbf{u}_p e^{j\mathbf{k}\cdot\mathbf{r}}. \tag{2}$$

The unit vector $\mathbf{u}_p$ is either $\mathbf{u}_\theta$ or $\mathbf{u}_\phi$, while $\mathbf{k} = k_0\mathbf{u}_k = k_x\mathbf{u}_x + k_y\mathbf{u}_y + k_z\mathbf{u}_z$ with $k_x = k_0 \sin\theta\cos\phi$, $k_y = k_0 \sin\theta \sin\phi$, and $k_z = k_0 \cos\theta$ (k_0 is the free-space wavenumber, i.e., $k_0 = 2\pi/\lambda_0 = 2\pi f/c$ where λ_0 is the free-space wavelength and c is the speed of light in vacuum). The reciprocity theorem can also be used to show that the elementary dipole along the y direction, considered in this paper, cannot excite TEM waves traveling along the wires, because the dipole is orthogonal to the field of the TEM waves [29].

The power density per unit solid angle P (W/sterad) is then obtained as

$$P(\theta, \phi) = \frac{1}{2\eta_0}\left[\left|E_\theta^{\mathrm{ff}}(\theta, \phi)\right|^2 + \left|E_\phi^{\mathrm{ff}}(\theta, \phi)\right|^2\right]. \tag{3}$$

The grounded wire-medium slab is modeled here as a homogeneous non-magnetic slab of thickness h (see Fig. 1). The choice of the parameter h is non-trivial: due to the presence of fringe fields above and below the top and bottom wire layers, h must be suitably higher than the physical thickness $(N-1)d + 2a$; here we let $h = Nd$, a simple choice that was shown in [30] to be optimal for modeling plane-wave reflection and transmission through wire-medium slabs in air.

The spectral dyadic permittivity of the homogenized wire medium is [16]

$$\begin{aligned}\underline{\underline{\varepsilon}} &= \varepsilon_0[\kappa_1 \mathbf{u}_y\mathbf{u}_y + \kappa_2(\mathbf{u}_x\mathbf{u}_x + \mathbf{u}_z\mathbf{u}_z)] \\ &= \varepsilon_0\varepsilon_{\mathrm{rh}}\left[\left(1 - \frac{{k_{\mathrm{p}}}^2}{\varepsilon_{\mathrm{rh}}{k_0}^2 - {k_y}^2}\right)\mathbf{u}_y\mathbf{u}_y + \mathbf{u}_x\mathbf{u}_x + \mathbf{u}_z\mathbf{u}_z\right].\end{aligned} \tag{4}$$

In (4), $k_{\mathrm{p}} = 2\pi f_{\mathrm{p}}/c$ is the plasma wavenumber, where f_{p} is the plasma frequency of the homogenized medium when the wires are embedded in free space and $k_y = 0$ (since in such a case the permittivity reduces to a scalar quantity that is formally the same as the dielectric permittivity of a plasma medium). An

approximate expression for $f_{\rm P}$ as a function of the wire radius a and the wire spacing d (see Fig. 1) is

$$f_{\rm P} = \frac{c}{d}\frac{1}{\sqrt{2\pi\left(\ln\frac{d}{2\pi a}+0.5275\right)}} \tag{5}$$

valid for $a \ll d \ll \lambda_0$ [16].

The homogenized wire medium is thus uniaxial and the dependence of the permittivity $\underline{\underline{\varepsilon}}$ on k_0 and k_y in (4) indicates the presence of both temporal and spatial dispersion, respectively. In the following subsections it will be shown that the spatial dispersion plays a crucial role in producing the peculiar radiation features of the considered structure, and in particular the omnidirectional nature of the radiated beam.

A. Transverse Equivalent Network (TEN)

The field can be decomposed into its TE_y and TM_y parts, which correspond to ordinary and extraordinary waves, respectively, inside the slab medium [29]. As noted in [16], for the considered spatially-dispersive uniaxial medium the effective refractive indices for both ordinary and extraordinary plane waves are independent of their propagation directions, and are equal to $n_{\rm o} = \sqrt{\varepsilon_{\rm rh}}$ and $n_{\rm e} = \sqrt{\varepsilon_{\rm rh} - {k_{\rm p}}^2/{k_0}^2}$, respectively.

The $\mathrm{TE}_y/\mathrm{TM}_y$ fields inside the wire-medium slab as well as in free space can be modeled using equivalent transmission lines (TLs) along the vertical z axis, starting from the spectral form of Maxwell's equations (an alternative derivation based on Hertz vector potentials is given in [29, Sec. 3.7]). This TEN model is valid for plane-wave incidence on the slab structure (used in the reciprocity calculation of the far field from the dipole source) as well as for the analysis of modal propagation on the wire-medium slab. In the TEN, the voltage on the TE line models E_x for the TE_y wave, while the voltage on the TM line models E_y for the TM_y wave.

The air-slab interface is represented by a four-port network, obtained by enforcing the continuity of the tangential components of the electric and magnetic fields at the interface (see [29, Sec. 3.7]). It should be noted that, since the wires are parallel to the air-slab interface, no additional boundary conditions are required; these should be introduced, e.g., in the case of wires orthogonal to the interface, as a consequence of the spatially-dispersive nature of the wire medium [31]. The complete TEN for the present problem is then the one shown in Fig. 2, where the network parameters are

$$\begin{aligned}
\hat{k}_{z1} &= \hat{k}_{z2} = \sqrt{1-\hat{k}_x^2-\hat{k}_y^2}\\
\hat{k}_{z3} &= \sqrt{{n_{\rm o}}^2-\hat{k}_x^2-\hat{k}_y^2},\\
\hat{k}_{z4} &= \sqrt{{n_{\rm e}}^2-\hat{k}_x^2-\hat{k}_y^2}
\end{aligned} \tag{6}$$

and

$$\begin{aligned}
\hat{Z}_{\rm c1} &= \frac{\hat{k}_{z1}}{1-\hat{k}_y^2}, \hat{Z}_{\rm c2} = \frac{1-\hat{k}_y^2}{\hat{k}_{z2}}\\
\hat{Z}_{\rm c3} &= \frac{\hat{k}_{z3}}{\varepsilon_{\rm rh}-\hat{k}_y^2}, \hat{Z}_{\rm c4} = \frac{\varepsilon_{\rm rh}-\hat{k}_y^2}{\varepsilon_{\rm rh}\hat{k}_{z4}}
\end{aligned} \tag{7}$$

where $\hat{k}_x = \sin\theta\cos\phi$ and $\hat{k}_y = \sin\theta\sin\phi$.

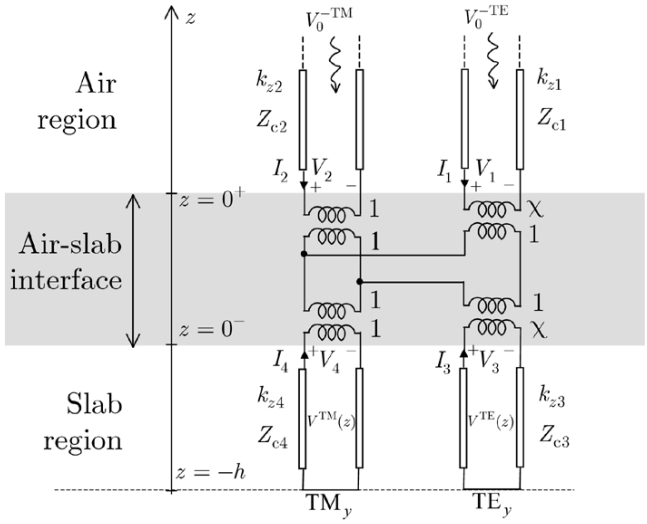

Fig. 2. Transverse equivalent network (TEN) for the problem of plane-wave incidence shown in Fig. 1

The coupling parameter χ, which is the turns ratio of the transformers connected at the TE_y ports 1 and 3 of the four-port network (see Fig. 2), depends on the incidence angle of the impinging plane wave as

$$\chi = \frac{(\varepsilon_{\rm rh}-1)\,\hat{k}_x\hat{k}_y}{\left(1-\hat{k}_y^2\right)\left(\varepsilon_{\rm rh}-\hat{k}_y^2\right)}. \tag{8}$$

This is equal to zero for incidence in the principal planes $\phi = 0°$ and $\phi = 90°$ (H and E planes), or for any incidence angle when $\varepsilon_{\rm rh} = 1$; in these cases, there is no $\mathrm{TE}_y/\mathrm{TM}_y$ coupling at the air-slab interface.

The incident voltages are proportional to the incident plane wave as $V_0^{\rm TM} = E_0\mathbf{u}_p\cdot\mathbf{u}_y$ and $V_0^{\rm TE} = \hat{Z}_{\rm c1}E_0\mathbf{u}_k\times\mathbf{u}_p\cdot\mathbf{u}_y$. The radiated power is evaluated via (1)–(3) where

$$E_y^{\rm pw}(\theta,\phi) = V^{\rm TM}(z_{\rm s}) \tag{9}$$

and $z_{\rm s} = -(h-h_{\rm s})$.

B. Radiation Features of a Homogenized Wire-Medium Slab

From the analysis in [10] we know that, when the wire-medium slab is excited by an electric line source parallel to the wire (y) axis, a directive broadside beam is radiated in the xz plane when $h = \lambda_\varepsilon/2$ (where λ_ε is the wavelength of the extraordinary wave inside the homogenized wire medium, i.e., $\lambda_\varepsilon = \lambda_0/n_{\rm e}$) and maximum broadside power density is obtained by letting $h_{\rm s} = h/2$. On the other hand, when the slab is excited by a horizontal electric dipole source parallel to the wire axis, a simple reasoning shows that the far field radiated in the xz plane (i.e., the H plane) is the same as the far field radiated in the same plane by the line source to within a constant factor; in fact, in both cases the far field can be computed through the reciprocity theorem as mentioned above, the only difference between the two cases being the amplitude of the electric field of the incident plane wave, which is $E_0 = \eta_0\sqrt{jk_0/(8\pi)}$

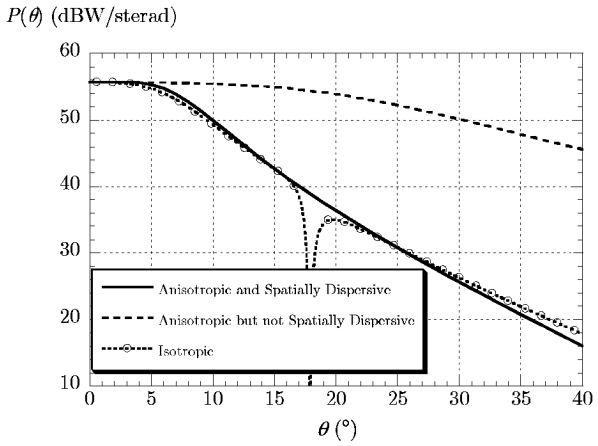

Fig. 3. Radiation patterns in the E plane of a wire-medium slab excited by a horizontal electric dipole as in Fig. 1, calculated with different homogeneous models for the slab. *Parameters*: $h = 120$ mm, $h_{\rm s} = h/2, \varepsilon_{\rm rh} = 1, f_{\rm p} = 3.88$ GHz, $f = 4.07$ GHz.

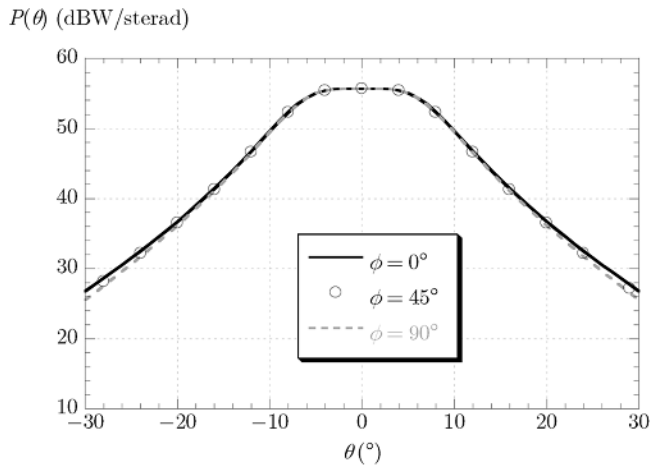

Fig. 4. Normalized radiation patterns in the principal planes for a horizontal electric dipole embedded in a grounded wire-medium slab. *Parameters* as in Fig. 3.

for the line source (see [10]) and $E_0 = -j\eta_0 k_0/(4\pi)$ for the dipole. Hence, the conditions $h = \lambda_\varepsilon/2$ and $h_{\rm s} = h/2$ give rise to a directive broadside beam with maximum broadside power density also for the dipole excitation (since broadside may be viewed as a special case of the H-plane pattern).

The radiation pattern produced by the infinitesimal electric dipole in the E plane $\phi = 90°$ (or in any other elevation plane different from the H plane) cannot be deduced from the analysis of the line-source excitation, and must be computed directly through the TEN described in the previous subsection. In order to illustrate the role of anisotropy and of spatial dispersion in shaping the beam radiated by a horizontal electric dipole inside a homogenized wire-medium slab, Fig. 3 shows three radiation patterns in the E plane for a structure as in Fig. 1 with $N = 6$ periodic layers of cylinders with radius $a = 0.5$ mm and spatial period $d = 20$ mm. The wire medium is modeled as i) an isotropic medium with scalar relative permittivity $\varepsilon_{\rm r} = \varepsilon_{\rm rh} - f_{\rm p}^2/f^2$ (*dashed line with circles*); ii) a uniaxial anisotropic medium with optical axis along y and principal relative permittivities $\kappa_1 = \varepsilon_{\rm rh} - f_{\rm p}^2/f^2$ (along y) and $\kappa_2 = \varepsilon_{\rm rh}$ (along x and z) (*dashed line*); and iii) a uniaxial anisotropic and spatially-dispersive medium with dyadic permittivity as in (4) (*solid line*); the plasma frequency is $f_{\rm p} = 3.88$ GHz (see (5)) and the relative permittivity of the host medium is $\varepsilon_{\rm rh} = 1$; the equivalent thickness is $h = Nd = 120$ mm and $h_{\rm s} = h/2$. The radiated power density in watts per steradian is shown in dB, relative to one watt per steradian. It can be noted that the anisotropic, but not spatially-dispersive, model produces a much wider beam than the isotropic model. The introduction of spatial dispersion in the anisotropic model produces an evident narrowing of the beam, which becomes almost equal to the beam obtained in the isotropic case (except for the absence of a narrow dip occurring at $\theta \simeq 18°$, where the level of radiation is anyway much lower than at broadside). Although Fig. 3 shows the role of spatial dispersion in narrowing the beam, it is not intended as a validation of the homogenization process, that will be demonstrated later by comparisons with full-wave simulations.

A ray-optics explanation that partially accounts for the high directivity is based on observing that rays emitted by the source refract at the interface between wire medium and air, and produce rays in the air region confined in a narrow angular range close to broadside [6], [25]. This happens for the isotropic as well as for the anisotropic and spatially-dispersive models, whereas they are spread out in the entire angular range for the anisotropic but not spatially-dispersive model. However, a more complete explanation of the underlying radiation mechanism, that takes into account the multiple bounces of the rays inside the grounded slab, is provided by the properties of the leaky modes presented in Section V.

In Fig. 4, radiation patterns in the principal planes $\phi = 0°$ (H plane), $\phi = 45°$ (D plane), and $\phi = 90°$ (E plane) are presented for a structure as in Fig. 3 [modeled through (4)] at the optimum frequency $f = 4.07$ GHz for which the broadside power density is maximum (an approximate formula for the optimum frequency is given in [10]). The three radiation patterns are almost identical, showing that the considered wire medium is a promising candidate for obtaining narrow *omnidirectional* pencil beams pointing at broadside, employing a simple finite source.

III. Full-Wave Analysis Via Method of Moments

In order to validate the results obtained with the homogenized model of the wire-medium slab, actual periodic metamaterial slabs have been simulated with air as the host medium, i.e., $\varepsilon_{\rm rh} = 1$.

The radiation pattern produced by a y-directed dipole source has been calculated by means of the reciprocity theorem as in Section II, considering a plane wave incident on the periodic structure and calculating the y-directed electric field at the source location. The current excited on the metal cylinders has been calculated with a method of moments (MoM) discretization of the relevant electric-field integral equation. The periodicity along the x direction allows us to consider only one spatial period (*unit cell*) of the structure, employing a one-dimensional periodic Green's function, suitably accelerated with the Ewald method [33]. Pulse current basis function directed along y are used, defined on a polygonal approximation of the circular cross-section of the wires. Since the electric

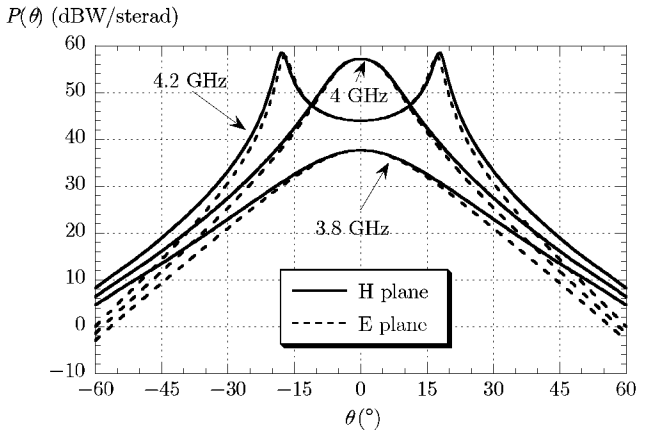

Fig. 5. Radiation patterns (in dB with respect to one W/sterad) for a horizontal electric dipole embedded in a grounded wire-medium slab. MoM results with $N = 6$ layers, $a = 0.5$ mm, $d = 20$ mm, $h_s = h/2$.

dipole source is parallel to the cylinder axis and $\varepsilon_{rh} = 1$, the excited field is purely TM with respect to the axis of the wires. Furthermore, the translational symmetry of the structure along the y direction and the homogeneity of the host medium allows for the calculation of the current on the cylinders for an *arbitrary* direction of propagation of the incident plane wave (2.5D problem) by suitably modifying a code written for the *normal*-incidence case (2D problem). Details of this procedure are given in Appendix I.

In Fig. 5, results for the radiation patterns in the principal planes are reported for a structure with $N = 6$ periodic layers of cylinders with radius $a = 0.5$ mm and spatial period $d = 20$ mm (this structure corresponds to the homogenized structure considered in Figs. 3 and 4 having $f_p = 3.88$ GHz). The dipole source is placed in the middle of the slab ($h_s = h/2$), equidistant from the four nearest cylinders. In particular, three frequencies are considered, i.e., $f = 3.8$ GHz, $f = 4$ GHz, and $f = 4.2$ GHz. At the first two frequencies, a pattern pointing at broadside is obtained. At each frequency, the radiation pattern has the same beamwidth in the two principal planes. This confirms the possibility to achieve almost omnidirectional directive radiation at broadside, as expected from the results obtained in the previous section through the approximate procedure based on the homogenization of the wire medium. The result at $f = 4.2$ GHz shows a conical beam, with a maximum at $\theta \simeq 18°$; again, the patterns in the principal planes are very similar, i.e., both the pointing angles and the beamwidths, as well as the level of the maxima, are almost the same. This confirms that almost omnidirectional *conical* beams can be radiated by a horizontal dipole source, a feature due to the spatial dispersion of the wire medium.

IV. Conical Beam Scanning

It is interesting to consider the beam scanning obtained by increasing the operating frequency with respect to the optimum frequency for broadside radiation. In Figs. 6 and 7, radiation patterns in the principal planes are shown for a structure as in Fig. 5 at different frequencies obtained through both the homogenized model [see Figs. 6(a) and 7(a)] and the full-wave

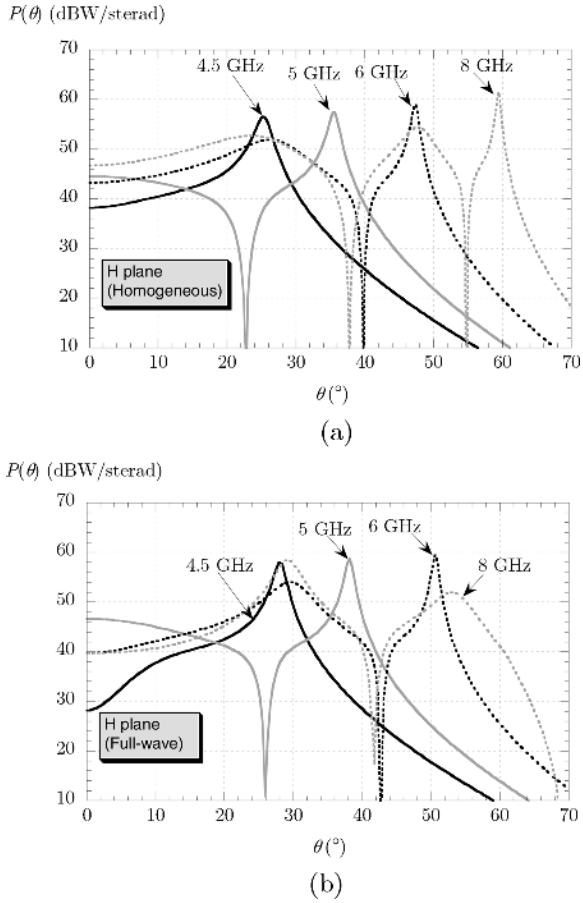

Fig. 6. Radiation patterns for a horizontal electric dipole embedded in a grounded wire-medium slab with parameters as in Fig. 5 at different operating frequencies in the H plane. (a) Homogeneous model, (b) full-wave MoM. *Homogenized-model parameters*: $h = 120$ mm, $h_s = h/2, \varepsilon_{rh} = 1, f_p = 3.88$ GHz.

approach [see Figs. 6(b) and 7(b)]. It can be seen that as the frequency increases, the main beam scans from broadside to endfire, and secondary lobes start to appear from broadside. These are typical features of leaky-wave radiation and, in particular, the secondary lobes are due to the excitation of higher-order leaky modes (the role of leaky waves will be illustrated in more detail in Section V).

As concerns the agreement between the homogenized model and the full-wave results, it can be noted that it is very good and independent of the observation angle in the E plane, while it tends to deteriorate for large observation angles and for high frequencies in the H plane, where a substantial difference is found at 8 GHz. This can be explained observing that, when the scan angle is increased in the H plane, the wavelength of the incident field in the x direction (i.e., in the direction of periodicity orthogonal to the wires) decreases, thus progressively reducing the validity of the homogenization procedure since the ratio of the spatial period to the transverse wavelength becomes larger. On the other hand, when the scan angle is increased in the E plane, the wavelength of the incident field decreases only in the y direction (i.e., parallel to the wires), along which the structure is translationally invariant; hence, in this case the validity of the homogenization procedure is not affected.

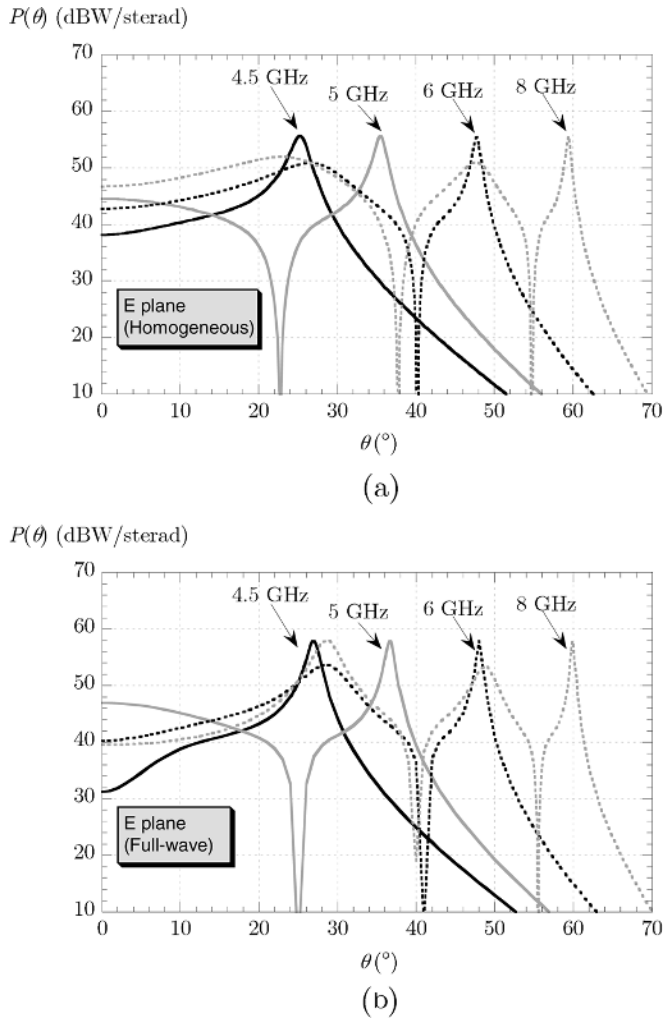

Fig. 7. As in Fig. 6 in the E plane.

During the scanning process, the beam angle and the beamwidth in the principal planes remain equal to each other; however, the peak field value increases in the H plane (see Fig. 6) but remains constant in the E plane (see Fig. 7). For scan angles up to about 30 degrees the peak power radiated in the E- and H-planes is approximately equal, and hence almost perfectly azimuthally symmetric conical beams are obtained. These features are very remarkable and should be contrasted with the behavior of 2D leaky-wave antennas based on Fabry-Perot cavities with partially-reflecting surfaces (PRSs), in which the beamwidths in the principal planes (and thus the pattern bandwiths) are generally different when the beam is scanned off broadside [32]. Therefore, the conical beam radiated from the considered homogenized wire-medium slab exhibits a higher degree of omnidirectionality with respect to PRS-based structures. This is due to the special spatial dispersion of this medium, as will be seen in Section V.

It is also worth comparing these scanning features with those of an isotropic plasmonic grounded slab with $\varepsilon_{\rm r} = \varepsilon_{\rm rh} - {k_{\rm p}}^2/{k_0}^2$ excited by the same source. The radiation patterns in the H plane are equal to those calculated with the anisotropic and spatially dispersive model [see Fig. 6(a)],

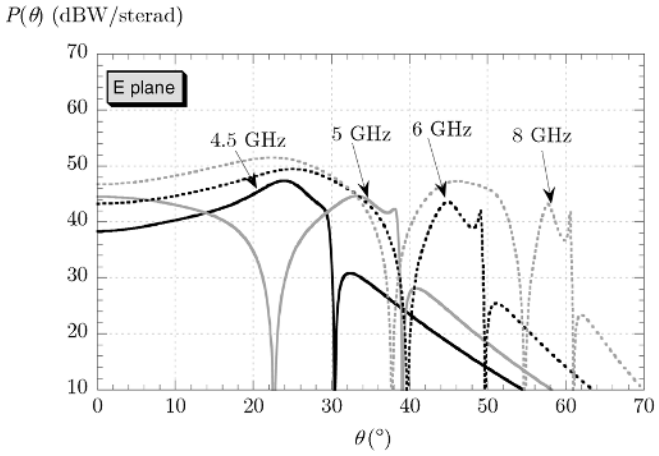

Fig. 8. As in Fig. 7(a) for an isotropic plasmonic grounded slab with $\varepsilon_{\rm r} = \varepsilon_{\rm rh} - {k_{\rm p}}^2/{k_0}^2$.

since the TM_y plane wave impinging on the wire-medium slab with $k_y = 0$, considered in the calculation of the pattern via reciprocity, has the electric field parallel to the wires and thus sees the medium as being effectively isotropic [see (4)]. On the other hand, the scanning process in the E plane, illustrated in Fig. 8, is dramatically different, due to the different characteristic impedance of the equivalent TL inside the slab; while a good agreement between the purely isotropic and the anisotropic-spatially dispersive models had been found when the beam points at broadside (see Fig. 3), a progressive degradation of the beam can be observed in Fig. 8 as the frequency (and hence the scan angle) is increased, with increasing levels of secondary lobes and the occurrence of undesired nulls.

V. Leaky Modes

In this section the radiative features illustrated in Sections II–IV are explained in terms of leaky modes supported by the grounded wire-medium slab, adopting both a homogenized model as in Section II and a MoM full-wave analysis as in Section III.

A. Analysis Via Homogenization

It is known from previous studies (see [10]) that in the 2D problem of a wire-medium slab excited by a line source the enhanced broadside directivity (achieved when $h = \lambda_\varepsilon/2$ and $h_{\rm s} = h/2$) is due to the excitation of a TE_{xz} leaky mode (this notation means that the mode is both TE_x and TE_z, since the electric field is in the y direction). This leaky mode has equal, and small, values for the phase and attenuation constants. In the present 3D configuration, radially-propagating cylindrical leaky waves have to be considered instead.

The TEN in Fig. 2 is used to determine the (generally complex) wavenumber $k_\rho = \beta - j\alpha$ of a mode traveling along the slab as $\exp[-jk_\rho(x\cos\phi + y\sin\phi)]$, at an angle ϕ with respect to the x axis. The analysis is carried out without plane-wave excitation, searching for the eigenmodes. The semi-infinite TLs in the air region of Fig. 2 can be replaced by their characteristic impedances, and the modal dispersion equation can be found

by enforcing the transverse resonance condition of the resulting network. The result is

$$[\hat{Z}_{c1} + j\hat{Z}_{c3}\tan(k_{z3}h)][\hat{Z}_{c2} + j\hat{Z}_{c4}\tan(k_{z4}h)] + \chi^2\hat{Z}_{c2}\hat{Z}_{c4} = 0 \quad (10)$$

where the normalized characteristic impedances $\hat{Z}_{ci}, i = 1,\dots 4$ can be calculated according to (6) and (7) with $\hat{k}_x = \hat{k}_\rho\cos\phi$ and $\hat{k}_y = \hat{k}_\rho\sin\phi$ (and $\hat{k}_\rho = k_\rho/k_0$). It can be noted that, in the absence of $\mathrm{TE}_y/\mathrm{TM}_y$ coupling at the air-slab interface (i.e., when $\chi = 0$), (10) can be factored into the product of two dispersion equations for purely TE_y modes ($[\hat{Z}_{c1} + j\hat{Z}_{c3}\tan(k_{z3}h)] = 0$) and purely TM_y modes ($[\hat{Z}_{c2} + j\hat{Z}_{c4}\tan(k_{z4}h)] = 0$). In the presence of $\mathrm{TE}_y/\mathrm{TM}_y$ coupling (i.e., when $\chi \neq 0$) the slab modes are generally hybrid. Leaky modes are found by choosing the improper determination for the vertical wavenumbers $\hat{k}_{z1} = \hat{k}_{z2} = \sqrt{1-\hat{k}_\rho^2}$, i.e., the one with a positive imaginary part, corresponding to fields that grow exponentially at infinity in the positive transverse z direction. The improper nature is typical for a leaky wave. This well-known property does not mean that the leaky mode is non-physical, since the leaky-mode fields excited by a source only exist within an angular region of space, defined by the phase constant (see [34] for more details).

We consider first the case of wires in vacuum, i.e., $\varepsilon_{\mathrm{rh}} = 1$. Since $\chi = 0$, according to the above discussion TE_y and TM_y modes can exist separately. Since a TE_y field does not interact with the wires and 'sees' an equivalent permittivity equal to that of the host medium, for such a polarization the slab simply does not exist; hence no TE_y modes can be supported by the structure. On the other hand, the dispersion equation for TM_y modes becomes

$$0 = \hat{Z}_{c2} + j\hat{Z}_{c4}\tan(k_{z4}h) = \frac{1-\hat{k}_y^2}{\hat{k}_{z2}\hat{k}_{z4}}[\hat{k}_{z4} + j\hat{k}_{z2}\tan(k_{z4}h)]. \quad (11)$$

The dispersion equation can be reduced by equating to zero the bracketed term in (11) which, most remarkably, *does not depend* on the mode propagation angle ϕ, since the vertical wavenumbers $\hat{k}_{z2}$ and $\hat{k}_{z4}$ only depend on the radial wavenumber k_ρ. This means that the leaky-mode wavenumber k_ρ is the same in all directions (in particular, when $\phi = 0°$ this mode is the TE_{xz} mode that would be excited by a line source in a 2D problem as considered in [10]). Therefore, in spite of the apparent directionality of the wire medium, propagation of TM_y (i.e., extraordinary) modes along the slab is omnidirectional. This can be seen actually as a direct consequence of the isotropy of extraordinary plane-wave propagation in an unbounded wire-medium space, pointed out in [16], taking into account that any modal field inside the slab can be decomposed into the sum of two plane waves bouncing between the ground plane and the air/wire-medium interface, and that no $\mathrm{TE}_y/\mathrm{TM}_y$ coupling occurs at that interface.

The omnidirectional leaky-wave propagation explains the radiative features found in the previous sections. In particular, the omnidirectionality of the beam radiated at broadside when $h = \lambda_\varepsilon/2$ is a direct consequence of the independence of the leaky-mode wavenumber of the azimuthal angle ϕ, so that the optimum condition $\beta = \alpha$ holds in all directions. When frequency is increased, we have that $\beta > \alpha$ (see Fig. 9) and the beam scans in all azimuthal planes with the same beam angle θ_{M}, since this is related to the leaky-mode phase constant ($\sin\theta_{\mathrm{M}} \simeq \beta/k_0$ when $\beta \gg \alpha$), and also with the same beamwidth $\Delta\theta_{3\mathrm{dB}}$, since this is related to the leaky-mode attenuation constant. In Fig. 9 the dispersion curves for the first three leaky modes of odd index (the modes are numbered according to increasing values of attenuation constant) for the structure considered in Figs. 6 and 7 are shown; in particular, it can be verified that at each frequency the pointing angle of the main beam in Figs. 6 and 7 is well predicted by the value of the phase constant of the dominant leaky mode (solid line 1 in Fig. 9), while the pointing angle of the secondary lobes is related to the values of the phase constants of the higher-order leaky modes (solid lines 3 and 5), thus further confirming the leaky-wave nature of the radiation. Although not reported in Fig. 9, it can be shown that the nulls in the radiation patterns in Figs. 6 and 7 are related to the leaky modes of even index [10]. Finally, it should be noted that since $\varepsilon_{\mathrm{rh}} = 1$, according to the above considerations, the dispersion behavior of the involved leaky modes is the same in all the azimuthal planes: in other words, β and α are ϕ-independent.

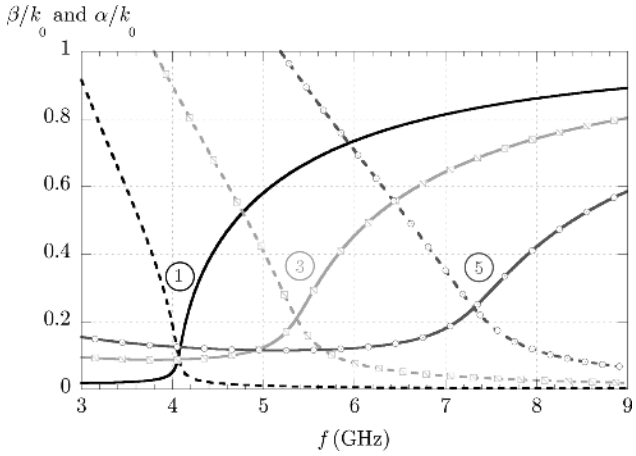

Fig. 9. Normalized phase (β/k_0) and attenuation (α/k_0) constants of the first three leaky modes of odd order supported by a wire-medium slab modeled as a homogeneous anisotropic spatially-dispersive medium, as a function of frequency. *Parameters* as in Figs. 6 and 7. *Legend*: *Solid line*: phase constant; *Dashed line*: attenuation constant.

It is interesting to compare this behavior with that of a dielectric-layer leaky-wave antenna, as studied in [35], which is also capable of producing either a pencil beam at broadside or a conical beam at some scan angle. For the dielectric-layer leaky-wave antenna the broadside pencil beam will also be omnidirectional, but the beam is now due to a pair of leaky modes, one TM_z and one TE_z, which determine the E- and H-plane patterns, respectively. For the wire-medium slab a single TM_y leaky mode determines the pattern in both planes. For a conical beam that is scanned off broadside, the beam angles and beamwidths will be different in the principal planes for the dielectric-layer leaky-wave antenna, becoming more different as the scan angle increases. Interestingly, the anisotropy and spatial

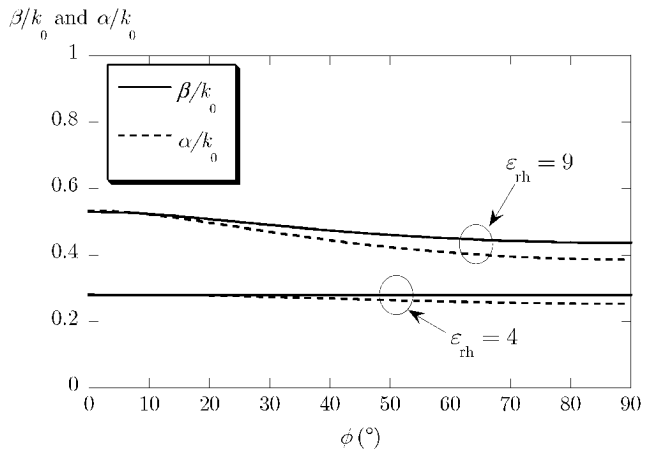

Fig. 10. Normalized phase (β/k_0) and attenuation (α/k_0) constants of the dominant leaky mode supported by two grounded wire-medium slabs modeled as homogeneous and anisotropic spatially-dispersive media, as a function of the propagation angle ϕ. *Parameters*: $h = 120$ mm, $f_{\rm p} = 3.88$ GHz, $\varepsilon_{\rm rh} = 4$ (and $f = 2.02$ GHz) or $\varepsilon_{\rm rh} = 9$ (and $f = 1.34$ GHz).

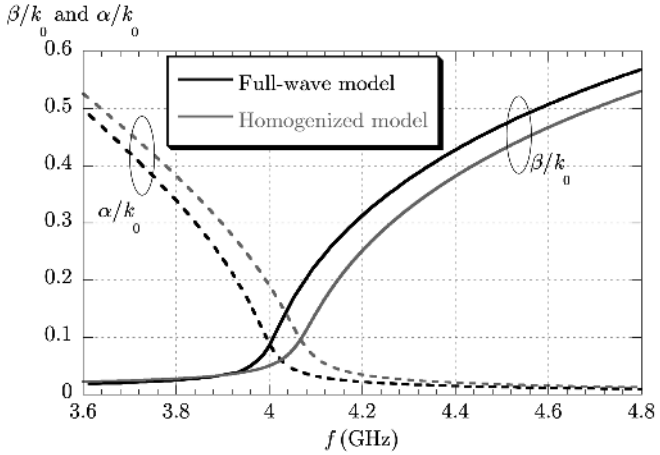

Fig. 11. Normalized phase (β/k_0) and attenuation (α/k_0) constants of the dominant leaky mode supported by a wire-medium slab: comparison between the homogenized model (*parameters* as in Figs. 6 and 7) and full-wave results (*parameters* as in Fig. 5).

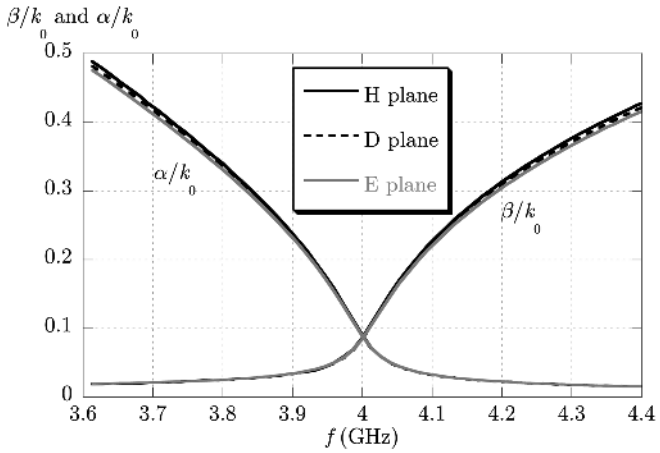

Fig. 12. Normalized phase (β/k_0) and attenuation (α/k_0) constants of the dominant leaky mode supported by a wire-medium slab as in Fig. 5, calculated with the full-wave approach for three propagation angles: $\phi = 0°$ (H plane), $\phi = 45°$ (D plane), and $\phi = 90°$ (E plane).

dispersion of the wire medium exactly compensates for the different propagation behavior in the principal planes that occurs with isotropic layers, leading to a completely omnidirectional propagation behavior.

When the host medium of the wires has $\varepsilon_{\rm rh} \neq 1$, the leaky-mode wavenumber k_ρ depends on the mode propagation angle ϕ. In Fig. 10 the wavenumber is reported as a function of ϕ for two slabs with $h = 120$ mm, $f_{\rm p} = 3.88$ GHz and $\varepsilon_{\rm rh} = 4$ or $\varepsilon_{\rm rh} = 9$, for the frequencies at which the phase and attenuation constants of the leaky mode are equal for propagation in the H plane $(\phi = 0°)$. A rather weak dependence of the wavenumber can be observed in both cases, due to the modest amount of $\mathrm{TE}_y/\mathrm{TM}_y$ coupling at the air-slab interface. The dominant leaky mode is a quasi-TM_y mode, whose complex wavenumber is shown in Fig. 10. In this case a quasi-TE_y mode also exists; however, it has a very large value of the attenuation constant, not shown here, so that it would not give any appreciable contribution to radiation.

B. Full-Wave Analysis

The method-of-moments procedure described in Section III for the calculation of the far-field patterns has also been employed to rigorously study the propagation of leaky modes along the actual periodic wire-medium slab. In this case the homogeneous (no excitation term) electric field integration equation (EFIE) is discretized, with the impedance matrix of the resulting linear system depending on the unknown modal wavenumber k_ρ. This is then found through a numerical root search for the complex zeros of the determinant of the impedance matrix.

In Fig. 11 a comparison is presented, for the case $\varepsilon_{\rm rh} = 1$, between the dispersion curves of the dominant TM_y leaky mode calculated with the homogeneous model and those calculated with the full-wave approach, for the same structures as in Figs. 6 (or 7) and 5, respectively, for propagation in the $\phi = 0°$ direction. A good overall agreement can be observed, although a frequency shift exists between the full-wave and homogenized results, which could in part be due to the choice of the equivalent homogenized-slab thickness h.

In Fig. 12 full-wave results are presented for the dispersion diagrams of the dominant TM_y leaky mode propagating in the principal directions $\phi = 0°$ (H plane), $\phi = 45°$ (D plane), and $\phi = 90°$ (E plane). As predicted by the homogenized model, when an actual wire medium is considered these dispersion curves are almost superimposed, thus confirming the omnidirectional nature of modal propagation along the wire-medium slab. It is interesting to note that this property can be established theoretically by considering the Green's function for the actual periodic grounded wire-medium slab [33] in the limit of vanishingly-small wire spacing: in fact, in this limit the modal wavenumber can be shown to become independent of the azimuthal angle ϕ. Hence, the omnidirectionality property of mode propagation, which is an exact property in the approximate homogenized model, turns out to be asymptotically exact (for vanishing period and wire radius) in the periodic model.

VI. Conclusion

In this paper the radiation from a dipole source embedded in a grounded wire-medium slab has been studied, with both a homogeneous model (which takes into account the anisotropy and the spatial dispersion of the effective medium) and a full-wave analysis of the actual structure via a periodic method-of-moments procedure.

The surprising characteristic of omnidirectional directive radiation is shown here for the first time and is interpreted in terms of a leaky mode supported by the structure. This explanation in terms of a leaky mode provides physical insight into the mechanism of radiation, it allows for a simple design rule (not discussed here) for determining the physical parameters of the structure in order to realize a given beamwidth, and it also allows for a simple estimation of the distance from the source at which the structure can be truncated with negligible edge-diffraction effects.

The results obtained with the full-wave analysis for both the radiation patterns and the dispersion behavior of the dominant leaky mode confirm the predictions of the homogenized model.

As a final remark, the idealized infinitesimal dipole considered here as a source provides a good model for practical feeds such as a short linear antenna or a printed dipole. It is worth noting that in this structure the source has mainly the role of a launcher for the relevant leaky mode responsible for the radiation pattern of the antenna. On the other hand, a study of the input impedance of a practical feed cannot be achieved with the simple homogenized model considered in this work, but would require a detailed calculation of the interaction between the source and the individual elements of the wire-medium lattice.

Appendix I
Integral-Equation Formulation for Oblique Incidence on PEC Cylinders

In this Appendix the integral-equation formulation for oblique incidence of a plane wave on a 2D PEC cylindrical structure is presented. In particular, it is shown how results for oblique incidence can simply be obtained from a method-of-moments code written for the normal-incidence case.

The EFIE for current on a single 2D PEC cylinder invariant along the y axis and illuminated by a field with y-variation of the form $e^{-jk_y y} = e^{-jk\cos\theta_y^{\rm inc} y}$ is

$$\left[jk\eta\int_{\mathcal{C}} G(k_\rho D)\tilde{\mathbf{J}}(\boldsymbol{\rho}')\mathrm{d}\ell' + -\frac{\eta}{jk}\tilde{\nabla}\int_{\mathcal{C}} G(k_\rho D)\tilde{\nabla}'\cdot\tilde{\mathbf{J}}(\boldsymbol{\rho}')\mathrm{d}\ell'\right]_{\tan} = \tilde{\mathbf{E}}^{\rm inc}_{\tan}(\boldsymbol{\rho}) \quad (12)$$

for $\boldsymbol{\rho}\in\mathcal{C}$. Here, $\mathbf{J}(\mathbf{r}) = \tilde{\mathbf{J}}(\boldsymbol{\rho}')e^{-jk_y y}$ is the surface current on the boundary $\mathcal{C}$ of the cylinder cross section, $\mathbf{E}^{\rm inc}(\mathbf{r}) = \tilde{\mathbf{E}}^{\rm inc}(\boldsymbol{\rho})e^{-jk_y y}$ is the incident electric field, $\mathbf{r} = \boldsymbol{\rho} + y\hat{\mathbf{y}}$, where $\boldsymbol{\rho} = x\hat{\mathbf{x}} + z\hat{\mathbf{z}}$, is the position vector, $G(k_\rho D) = H_0^{(2)}(k_\rho D)/(4j)$ is the Green's function for the 2D Helmholtz equation, $D = |\boldsymbol{\rho}' - \boldsymbol{\rho}|$ is the transverse distance between source and observation points, k and η are the wavenumber and the characteristic impedance of the medium surrounding the PEC cylinders, $k_\rho = (k^2 - k_y^2)^{1/2}$, $\tilde{\nabla} = \nabla_{\rm t} - jk_y\hat{\mathbf{y}}$, and ℓ is the direction tangential to $\mathcal{C}$.

In the TM_y case $J_\ell = 0$, thus (12) becomes, after projection onto the y and ℓ directions

$$\frac{\eta k_y}{k}\frac{\partial}{\partial\ell}\int_{\mathcal{C}} G(k_\rho D)\tilde{J}_y(\boldsymbol{\rho}')\mathrm{d}\ell' = E_\ell^{\rm inc}(\boldsymbol{\rho}) \quad (13)$$

$$jk_\rho\eta\int_{\mathcal{C}} G(k_\rho D)\tilde{J}_y(\boldsymbol{\rho}')\mathrm{d}\ell' = \frac{k}{k_\rho}E_y^{\rm inc}(\boldsymbol{\rho}). \quad (14)$$

The first equation of this pair is a dependent equation that actually follows from the second, as can be seen by applying the operator $(-jk_y/k_\rho^2)\partial/\partial\ell$ to both sides of the latter and using the fact that, for TM_y waves, $\mathbf{E}_{\rm t} = (-jk_y/k_\rho^2)\nabla_{\rm t}E_y$. The second is an integral equation for the TM_y current that differs only trivially from the normal incidence case, as discussed below.

If one uses the second integral equation to determine the current, then the y-component of the scattered electric field at a point $\boldsymbol{\rho}$ is given by

$$E_y^{\rm s}(\boldsymbol{\rho}) = -j\eta\frac{k_\rho^2}{k}\int_{\mathcal{C}} G(k_\rho D)\tilde{J}_y(\boldsymbol{\rho}')\mathrm{d}\ell' = -j\eta k_\rho\sin\theta_y^{\rm inc}\int_{\mathcal{C}} G(k_\rho D)\tilde{J}_y(\boldsymbol{\rho}')\mathrm{d}\ell' \quad (15)$$

Clearly the oblique incidence case differs from the normal incidence case only by an interchange of the symbols k_ρ and k. Note that the excitation term of the integral (14) does not need to be rescaled: the magnitude of the y-component of an incident plane wave field varies as $k_\rho/k = \sin\theta_y^{\rm inc}$ whereas the reciprocal of this factor appears as a multiplier of the incident field on the RHS of (14). Hence the excitation function is angle-independent. On the other hand, in computing the scattered electric field, the same wavenumber rescaling is used as in determining the current but, as (15) illustrates, the result should then be multiplied by the factor $k_\rho/k = \sin\theta_y^{\rm inc}$.

Finally, the possibility to treat the problem of oblique incidence of a plane wave on a periodic array of cylinders with a normal-incidence code can be established with a reasoning similar to the one presented above for the single-cylinder case, since the periodic case is simply a collection of cylinders, so that the contour $\mathcal{C}$ is now an infinite set of circular contours.

References

[1] K. C. Gupta, "Narrow-beam antennas using an artificial dielectric medium with permittivity less than unity," *Electron. Lett.*, vol. 7, pp. 16–18, Jan. 1971.

[2] I. J. Bahl and K. C. Gupta, "A leaky-wave antenna using an artificial dielectric medium," *IEEE Trans. Antennas Propag.*, vol. AP-22, pp. 119–122, Jan. 1974.

[3] G. Poilasne, P. Pouliguen, J. Lenormand, K. Mahdjoubi, C. Terret, and P. Gelin, "Theoretical study of interactions between antennas and metallic photonic bandgap materials," *Microw. Opt. Technol. Lett.*, vol. 15, pp. 384–389, Mar. 1997.

[4] M. Thèvenot, C. Cheype, A. Reineix, and B. Jecko, "Directive photonic bandgap antennas," *IEEE Trans. Microw. Theory Tech.*, vol. 47, pp. 2115–2122, Nov. 1999.

[5] B. Temelkuaran, M. Bayindir, E. Ozbay, R. Biswas, M. M. Sigalas, G. Tuttle, and K. M. Ho, "Photonic crystal-based resonant antenna with a very high directivity," *J. Appl. Phys.*, vol. 87, pp. 603–605, 2000.
[6] S. Enoch, G. Tayeb, P. Sabouroux, N. Guérin, and P. Vincent, "A metamaterial for directive emission," *Phys. Rev. Lett.*, vol. 89, pp. 213902-1–-213902-4, Nov. 2002.
[7] T. Akalin, J. Danglot, O. Vanbésien, and D. Lippens, "A highly directive dipole antenna embedded in a Fabry-Pérot type cavity," *IEEE Microw. Wireless Comp. Lett.*, vol. 12, no. 2, pp. 48–50, Feb. 2002.
[8] H. Boutayeb, K. Mahdjoubi, A.-C. Tarot, and T. A. Denidni, "Directivity of an antenna embedded inside a Fabry-Perot cavity: Analysis and design," *Microw. Opt. Techn. Lett.*, vol. 48, pp. 12–17, Jan. 2006.
[9] N. Guèrin, S. Enoch, G. Tayeb, P. Sabouroux, P. Vincent, and H. Legay, "A metallic Fabry-Perot directive antenna," *IEEE Trans. Antennas Propag.*, vol. 54, pp. 220–224, Jan. 2006.
[10] G. Lovat, P. Burghignoli, F. Capolino, D. R. Jackson, and D. R. Wilton, "Analysis of directive radiation from a line source in a metamaterial slab with low permittivity," *IEEE Trans. Antennas Propag.*, vol. 54, pp. 1017–1030, Mar. 2006.
[11] Y. J. Lee, W. S. Park, J. Yeo, and R. Mittra, "Directivity enhancement of printed antennas using a class of metamaterial superstrates," *Electromagn.*, vol. 26, pp. 203–218, Apr. 2006.
[12] A. Alu, F. Bilotti, N. Engheta, and L. Vegni, "Metamaterial covers over a small aperture," *IEEE Trans. Antennas Propag.*, vol. 54, pp. 1632–1643, Jun. 2006.
[13] J. Brown, "Artificial dielectrics having refractive indices less than unity," *Proc. Inst. Elect. Eng.*, vol. 100, pp. 51–62, May 1953.
[14] R. N. Bracewell, "Analogues of an ionized medium: Applications to the ionosphere," *Wireless Engr.*, vol. 31, pp. 320–326, Dec. 1954.
[15] W. Rotman, "Plasma simulation by artificial dielectrics and parallel-plate media," *IRE Trans. Antennas Propag.*, vol. AP-10, pp. 82–95, Jan. 1962.
[16] P. A. Belov, R. Marqués, S. I. Maslovski, I. S. Nefedov, M. Silveirinha, C. R. Simovski, and S. A. Tretyakov, "Strong spatial dispersion in wire media in the very large wavelength limit," *Phys. Rev. B*, vol. 67, pp. 113103-1–113103-4, 2003.
[17] C. A. Moses and N. Engheta, "Electromagnetic wave propagation in the wire medium: A complex medium with long thin inclusions," *Wave Mot.*, vol. 34, pp. 310–317, 2001.
[18] P. A. Belov, C. R. Simovski, and S. A. Tretyakov, "Two-dimensional electromagnetic crystals formed by reactively loaded wires," *Phys. Rev. E*, vol. 66, pp. 036610-1–036610-7, Sep. 2002.
[19] C. R. Simovski and P. A. Belov, "Low-frequency spatial dispersion in wire media," *Phys. Rev. E*, vol. 70, pp. 046616-1–046616-8, Oct. 2004.
[20] M. G. Silveirinha and C. A. Fernandes, "Homogenization of 3-D-connected and nonconnected wire metamaterial," *IEEE Trans. Microw. Theory Tech.*, vol. 53, no. 4, pp. 1418–1430, Apr. 2005.
[21] M. G. Silveirinha and C. A. Fernandes, "Homogenization of metamaterial surfaces and slabs," *IEEE Trans. Antennas Propag.*, vol. 53, no. 1, pp. 59–69, Jan. 2005.
[22] I. S. Nefedov, A. J. Viitanen, and S. A. Tretyakov, "Propagating and evanescent modes in two-dimensional wire media," *Phys. Rev. E*, vol. 71, pp. 046612-1–046612-10, 2005.
[23] I. S. Nefedov and A. J. Viitanen, "Guided waves in uniaxial wire medium slab," *PIER*, vol. 51, pp. 167–185, 2005.
[24] D. Bonefacčić, S. Hrabar, and D. Kvakan, "Experimental investigation of radiation properties of an antenna embedded in low-permittivity thin-wire-based metamaterials," *Microw. Opt. Technol. Lett.*, vol. 48, no. 12, pp. 2581–2586, Dec. 2006.
[25] G. Lovat, P. Burghignoli, F. Capolino, and D. R. Jackson, "High directivity in low-permittivity metamaterial slabs: Ray-optic vs. leaky-wave models," *Microw. Opt. Technol. Lett.*, vol. 48, no. 12, pp. 2542–2548, Dec. 2006.
[26] G. Lovat, P. Burghignoli, F. Capolino, and D. R. Jackson, "On the combinations of low/high permittivity and/or permeability substrates for highly-directive planar metamaterial antennas," *IET Microw. Antennas Propag., Special Issue on Metamaterials LHM and Metamaterials EBG*, vol. 1, no. 1, pp. 177–183, Feb. 2007.
[27] G. Lovat, P. Burghignoli, F. Capolino, and D. R. Jackson, "Highly-directive planar leaky-wave antennas: A comparison between metamaterial-based and conventional designs," *Proc. Eur. Microw. Association*, vol. 2, no. 1, pp. 12–21, Mar. 2006.
[28] D. R. Jackson and N. G. Alexópoulos, "Gain enhancement methods for printed circuit antennas," *IEEE Trans. Antennas Propag.*, vol. AP-33, pp. 976–987, Sep. 1985.
[29] R. E. Collin, *Field Theory of Guided Waves*, 2nd ed. Piscataway, NJ: IEEE Press, 1991.
[30] G. Guida, D. Maystre, G. Tayeb, and P. Vincent, "Mean-field theory of two-dimensional metallic photonic crystals," *J. Opt. Soc. Am. B*, vol. 15, pp. 2308–2315, 1998.
[31] M. G. Silveirinha, "Additional boundary condition for the wire medium," *IEEE Trans. Antennas Propag.*, vol. 54, no. 6, pp. 1766–1780, Jun. 2006.
[32] T. Zhao, D. R. Jackson, J. T. Williams, and A. A. Oliner, "General formulas for 2-D leaky-wave antennas," *IEEE Trans. Antennas Propag.*, vol. 53, no. 11, pp. 3525–3533, Nov. 2005.
[33] F. Capolino, D. R. Wilton, and W. A. Johnson, "Efficient calculation of the 2-D Green's function for 1-D periodic structures using the Ewald method," *IEEE Trans. Antennas Propag.*, vol. 53, no. 9, pp. 2977–2984, Sep. 2005.
[34] T. Tamir and A. A. Oliner, "Guided complex waves. Part I: Fields at an interface. Part II: Relation to radiation patterns," *Proc. Inst. Elect. Eng.*, vol. 110, pp. 310–334, Feb. 1963.
[35] D. R. Jackson, A. A. Oliner, and A. Ip, "Leaky-wave propagation and radiation for a narrow-beam multiple-layer dielectric structure," *IEEE Trans. Antennas Propag.*, vol. 41, no. 3, pp. 344–348, Mar. 1993.

Paolo Burghignoli (S'97–M'01–SM'08) was born in Rome, Italy, on February 18, 1973. He received the Laurea degree (*cum laude*) in electronic engineering and the Ph.D. degree in applied electromagnetics, both from "La Sapienza" University of Rome, Rome, in 1997 and 2001, respectively.

In 1997, he joined the Electronic Engineering Department of "La Sapienza" University of Rome, where he is currently an Associate Researcher. From January 2004 to July 2004, he was a Visiting Research Assistant Professor at the University of Houston, Houston, TX. His scientific interests include analysis and design of planar leaky-wave antennas, numerical methods for the analysis of passive guiding and radiating microwave structures, periodic structures, and propagation and radiation in metamaterials.

Dr. Burghignoli received the Graduate Fellowship Award from the IEEE Microwave Theory and Techniques Society in 2003, the Raj Mittra Travel Grant for Junior Researchers from the 2005 Antennas and Propagation Symposium, Washington, DC, and the "Giorgio Barzilai" Laurea Prize from the former IEEE Central and South Italy Section in 2007.

Giampiero Lovat (S'02–M'06) was born in Rome, Italy, on May 31, 1975. He received the Laurea degree (*cum laude*) in electronic engineering and the Ph.D. degree in applied electromagnetics, both from "La Sapienza" University of Rome, Rome, in 2001 and 2004, respectively.

In 2005, he joined the Electrical Engineering Department of "La Sapienza" University of Rome, where he is currently an Associate Researcher. From January 2004 to July 2004, he was a Visiting Scholar at the University of Houston, Houston, TX. He is the coauthor of a book on electromagnetic shielding. His present research interests include leaky-wave antennas, periodic structures, complex media, and electromagnetic shielding.

Dr. Lovat received the Young Scientist Award from the 2005 URSI General Assembly, New Delhi, India.

Filippo Capolino (S'94–M'97–SM'04) was born in Florence, Italy, in 1967. He received the Laurea degree (*cum laude*) in electronic engineering and the Ph.D. degree, from the University of Florence, Florence, Italy, in 1993 and 1997, respectively.

He is currently an Assistant Professor in the Department of Information Engineering, University of Siena, Italy. From 1997 to 1998, he was a Fulbright Research Visitor with the Department of Aerospace and Mechanical Engineering, Boston University, Boston, MA, where he continued his research with a Grant from the Italian National Council for Research (CNR), from 1998 to 1999. From 2000 to 2001, he was a Research Assistant Visiting Professor with the Department of Electrical and Computer Engineering, University of

Houston, Houston, TX, where he is now an Adjunct Assistant Professor. From November to December 2003, he was an Invited Assistant Professor at the Institut Fresnel, Marseille, France. His research interests include theoretical and applied electromagnetics focused on high-frequency, short-pulse radiation, array antennas, periodic structures, numerical modelling, and metamaterials. He is the Coordinator of the Metamorphose EU Doctoral Programmes on Metamaterials.

Dr. Capolino was awarded an MMET'94 Student Paper Competition Award in 1994, the Raj Mittra Travel Grant for Young and Senior Scientists in 1996 and 2006, respectively, the "Barzilai" Prize for the best paper at the National Italian Congress of Electromagnetism (XI RiNEm) in 1996, and a Young Scientist Award for participating at the URSI International Symposium on Electromagnetic Theory in 1998. He received the R. W. P. King Prize Paper Award from the IEEE Antennas and Propagation Society for the Best Paper of the Year 2000, by an author under 36. He is an Associate Editor for the IEEE TRANSACTIONS ON ANTENNAS AND PROPAGATION and *Metamaterials*.

David R. Jackson (S'83–M'84–SM'95–F'99) was born in St. Louis, MO, on March 28, 1957. He obtained the B.S.E.E. and M.S.E.E. degrees from the University of Missouri, Columbia, in 1979 and 1981, respectively, and the Ph.D. degree in electrical engineering from the University of California, Los Angeles, in 1985.

From 1985 to 1991, he was an Assistant Professor in the Department of Electrical and Computer Engineering, University of Houston, Houston, TX, where, from 1991 to 1998, he was an Associate Professor and, since 1998, he has been a Professor. His present research interests include microstrip antennas and circuits, leaky-wave antennas, leakage and radiation effects in microwave integrated circuits, periodic structures, and EMC.

Dr. Jackson is presently serving as the Chair of the Transnational Committee of the IEEE AP-S Society, and as the Chair for URSI, U.S. Commission B. He is also on the Editorial Board of the IEEE TRANSACTIONS ON MICROWAVE THEORY AND TECHNIQUES. Previously, he has been the Chapter Activities Coordinator for the IEEE AP-S Society, a Distinguished Lecturer for the AP-S Society, an Associate Editor for the IEEE TRANSACTIONS ON ANTENNAS AND PROPAGATION, and a member of the AdCom for the AP-S Society. He has also served as an Associate Editor for *Radio Science*, the *International Journal of RF*, and *Microwave Computer-Aided Engineering*.

Donald R. Wilton (S'63–M'65–SM'80–F'87–LF'08) was born in Lawton, OK, on October 25, 1942. He received the B.S., M.S., and Ph.D. degrees from the University of Illinois, Urbana-Champaign, in 1964, 1966, and 1970, respectively.

From 1965 to 1968, he was with Hughes Aircraft Co., Fullerton, CA, engaged in the analysis and design of phased array antennas. From 1970 to 1983 he was with the Department of Electrical Engineering, University of Mississippi, and since 1983 he has been Professor of electrical engineering at the University of Houston, Houston, TX. From 1978 to 1979, he was a Visiting Professor at Syracuse University. During 2004 to 2005, he was a Visiting Scholar at the Polytechnic of Turin, Italy, the Sandia National Laboratories, and the University of Washington. He has authored or coauthored many publications, lectured, and consulted extensively. His primary research interest is in computational electromagnetics.

Dr. Wilton is a member of Commission B of URSI, in which he has held various offices including Chair of U.S. Commission B. He received the IEEE Third Millennium Medal. He has served the IEEE Antennas and Propagation Society as an Associate Editor of the IEEE TRANSACTIONS ON ANTENNAS AND PROPAGATION, as a Distinguished National Lecturer, and as a member of AdCom.